Geomechanics and Engineering, *Vol. 30, No. 4 (2022) 353-362*
https://doi.org/10.12989/gae.2022.30.4.353

Response of segmented pipelines subject to earthquake effects

Adil Yigit*

Istanbul Natural Gas Distribution Company (IGDAS), IGDAS Kavacik Hizmet Binasi, Beykoz, Istanbul, Türkiye

(*Received October 21, 2021, Revised May 10, 2022, Accepted July 23, 2022*)

Abstract. The seismic failure-prone region in Istanbul has been examined in terms of the segmented pipelines. Although some researchers have suggested that this territory should be left as a green land, many people continue to live in this area. This region is about 9-10 km away from the North Anatolian Fault Line. This fault zone is an active right-lateral strike-slip fault line in Turkey and an earthquake with a magnitude of 7.0-7.5 is expected in the Marmara Sea. Therefore, superstructures and infrastructures are under both land sliding risks and seismic risks in this area. Because there are not any pipeline-fault line intersection points in the region, in this study, it has been focused on the behaviors of the segmented (sewage or stormwater) pipelines subject to earthquake-induced permanent ground deformation and seismic wave propagation. Based on the elastic beam theory some necessary analyses have been carried out and obtained results of this approximation have been examined.

Keywords: earthquake; landslide; segmented pipeline; seismic wave propagation; underground construction

1. Introduction

Infrastructure safety is one of the most important subject of structural engineering (Apak *et al*. 2022). Buried pipelines, which are one of the main members of infrastructures, can be damaged by an earthquake due to permanent ground deformation (PGD), seismic wave propagation (SWP) or pipeline-fault line intersection (Xie *et al*. 2021, Castiglia *et al*. 2018, Wang *et al*. 2020, Yoon *et al*. 2020, Zhang *et al*. 2020). The subject of seismic hazards on segmented pipelines is one of the significant branches of lifeline safety. Some essential analysis have been caried out on behaviours of segmented pipeline subject to earthquake effects (Wham *et al*. 2017, Wham and Davis 2019, Wijaya *et al*. 2019, Banushi and Wham 2021, Londono and O'Rourke 2019, Toprak *et al*. 2019, O'Rourke and Londono 2016, Toprak *et al*. 2015, Shi 2015a). In this paper, because there is no pipeline-fault line intersection case in investigated region, the vulnerability of the segmented pipelines has been examined in terms of the PGD and SWP.

The finite element method is generally used to solve such problems, but in this study, besides investigating the regional situation, it is also aimed to obtain easy and useful equations that can be used in practice to predict the earthquake effects on these pipelines. Therefore, depending on the elastic beam theory, a new analytical approach has been developed to be able to calculate the earthquake effects on buried segmented pipelines. In this paper, firstly permanent ground deformation (PGD) has been described. Then, the calculation of amount of PGD has been explained, since it is one of the most important parameters of this problem. The case of soil-pipe interaction has been investigated because this interaction causes frictional forces at the pipe-soil interface. Depends on elastic beam theory mathematical models have been created and solved. As a result, according to regional geology, seismicity and pipe material necessary analysis have been carried out and the results have been examined.

1.1 Permanent Ground Deformation (PGD)

In general, PGD types are defined as surface faulting, landsliding, seismic settlement and lateral spreading due to liquefaction. Since the investigated region is a landslide-prone area, in this article, landslide risk has been taken into consideration. The damage potential of PGD on pipeline systems is closely related to the amount of ground displacement. Beside new programming technologies (Nanehkaran *et al*. 2021) and machine learning models (Liu *et al*. 2021), Newmark Sliding Block Model is frequently used to predict earthquake-induced ground displacement.

1.2 Amount of PGD according to Newmark Method

According to the Newmark Method ground displacement can be estimated based on the strong ground motion records (Fig. 1). In this approximation, ground described as a slippery block and it is assumed that this block has a critical acceleration (a_c) level that moves the block. According to Fig. 1, the block has critical acceleration level of 0.2 g and it doesn't slide before the X point because the acceleration values of previous points from X are less than the critical acceleration level. After the X point, the velocity-time graph is obtained by integrating the acceleration-time record that exceeds the ac level over time. Before the Y point, the velocity increases and after this point, even though the acceleration value decreases, the motion of the block continues due to its inertia. The movement stops at point Z. This process is repeated at all

*Corresponding author, Ph.D.
E-mail: adilyigit75@hotmail.com

ISSN: 2005-307X (Print), 2092-6219 (Online)

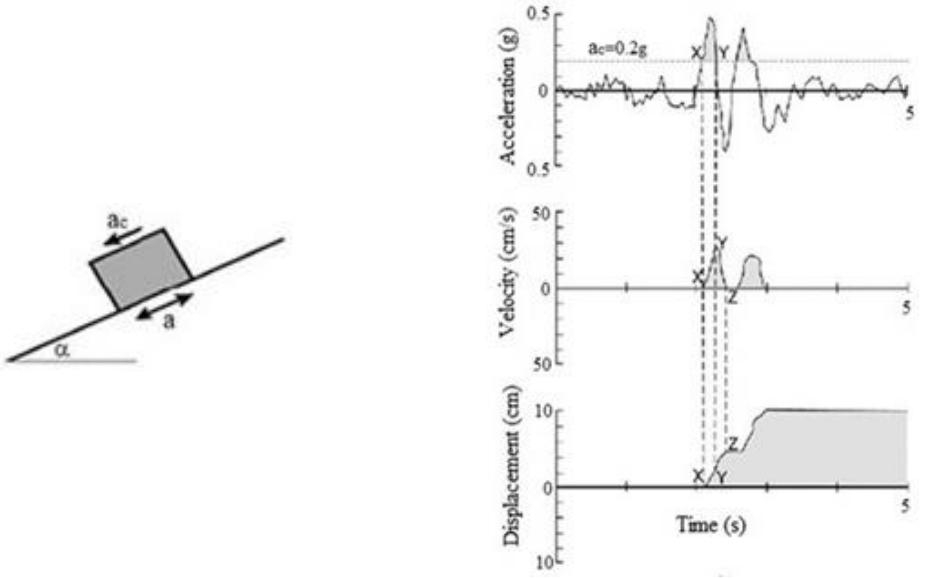

(a) Newmark sliding block model (b) Newmark analysis

Fig. 1 Newmark Method (Newmark1965)

other parts of the strong ground motion record where the acceleration value is over the critical acceleration level. As a result, the total movement of the block is obtained.

In literature, depends on this approximation some regression equations have been suggested to predict the earthquake-induced slope displacement (Ambraseys and Menu 1988, Jibson 1993, Jibson 1998, Jibson 2007, Hsieh and Lee 2011, Yigit 2020, 2021). To calculate Newmark Displacement, a regression equation commonly used in literature has been suggested by Jibson *et al*. (1998) as follows (Eq. (1))

$$log\delta = 1.521 log I_a - 1.993 log a_c - 1.546 \pm 0.375 \quad (1)$$

Where displacement (δ) is in cm, the critical acceleration (a_c) is in g and Arias intensity (I_a) is in m/s. To calculate Arias Intensity (m/s), Wilson and Keefer (1983) have suggested Eq. (2) depending on earthquake moment magnitude (M) and earthquake source distance (R, km)

$$log I_a = M - 2 log R - 4.1 \quad (2)$$

The critical acceleration (a_c) that triggers the movement of a slope has been described as Eq. (3) by Siyahi *et al*. (2003)

$$a_c = g\left[\frac{c}{\gamma h} + \cos\alpha \,.\, \tan\emptyset - \sin\alpha\right] \quad (3)$$

Ø is the effective friction angle, c is the effective cohesion, α is the slope angle, γ is the material unit weight, h is the slope-normal thickness of failure slab.

PGD, which can occur with seismic activity, is generally considered in two categories as spatially distributed and localized abrupt PGD. Abrupt permanent ground deformation has the same properties with a pipe-fault 900 angle crossing case (Fig. 2(b)). Spatially distributed PGD has been characterized by the width (W) and the amount of ground displacement (δ) as shown in the following figure (Fig. 2(a)).

O'Rourke (1989) has suggested the following equation

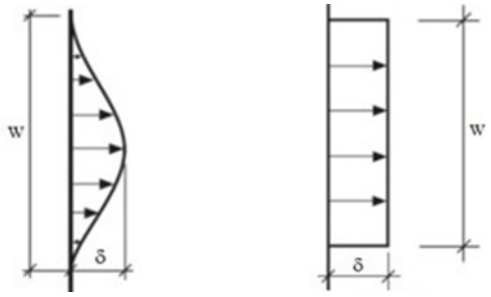

(a) Spatially distributed (b) Localized abrupt

Fig. 2 Transverse PGD types (O'Rourke 1989)

for spatially distributed transverse PGD

$$y(x) = \frac{\delta}{2}\left(1 - \cos\frac{2\pi x}{W}\right) \quad (4)$$

1.3 Seismic Wave Propagation (SWP)

Although PGD damages the pipeline locally, seismic wave propagation affects the entire pipeline system. However, PGD is more devastating than SWP. Seismic wave propagation hazards may occur because of strain and curvature of the ground due to traveling wave effects. SWP has been characterized by the wavelength, λ, and the wave amplitude, $\bar{\delta}$ (Fig. 3). Ground displacement has been explained as $U_x(x)$ for longitudinal direction and $U_y(x)$ for perpendicular direction. For strike-slip fault, Gregor (1995) has suggested an equation as Eq. (5) to calculate the seismic wave amplitude depending on the shortest distance to the fault line, R (km) and magnitude of the earthquake (M). V_s is the shear wave propagation velocity, T is the ground-period and Ø is the angle between the wave propagation direction and the pipeline axis (Yigit *et al*. 2018).

$$log\bar{\delta} = -5.0 + 1.02M - 0.87 log R \quad (5)$$

$$\lambda = V_s\, T \quad (6)$$

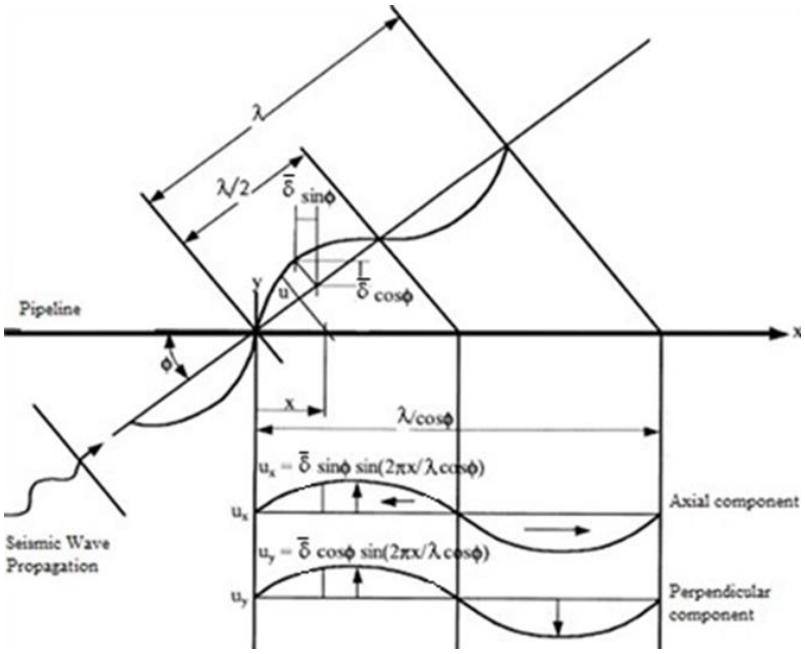

Fig. 3 Seismic wave propagation (Yigit *et al*. 2018)

$$u_x(x) = \bar{\delta} \sin \emptyset \sin\left(\frac{2\pi x}{\lambda} \cos \emptyset\right) \tag{7}$$

$$u_y(x) = \bar{\delta} \cos \emptyset \sin\left(\frac{2\pi x}{\lambda} \cos \emptyset\right) \tag{8}$$

1.4 Reaction of pipelines to PGD

In literature, many studies have been carried out to determine the reaction of pipelines to PGD. This problem is usually solved in two parts as transverse and longitudinal PGD case. Yigit *et al*. (2018) have described the problem as a beam on elastic soil foundation with built-in supports at both ends. According to spatially distributed ground displacement (Eq. (4)) pipeline displacement function has been obtained as below for transverse PGD case

$$v(x) = \frac{\delta}{2}\left(1 - e^{-\beta_v x} \cos \beta_v x\right) \tag{9}$$

The maximum strain due to axial force and bending moment (respectively ε_{at} and ε_b) have been defined as follows for continuous pipelines

$$\varepsilon_{at} = -1 + \sqrt{1 + \frac{\beta_v^2 \delta^2}{4}} \tag{10}$$

$$\varepsilon_b = \frac{\delta \beta_v^2 e^{\frac{-\pi}{4}}}{\sqrt{2}} \frac{D}{2} \tag{11}$$

D is the outside diameter of the pipe, δ is the ground displacement and it can be obtained from Eq. (1).

$$\beta_v = \sqrt[4]{\frac{k_v}{4EI}} \tag{12}$$

k_v is the transverse equivalent elastic soil spring coefficient. In the same study, the maximum strain caused by the longitudinal PGD has been described for continuous pipelines as follows (Yigit *et al*. 2018)

$$\varepsilon_{al} = \beta_u \sqrt{\frac{x_u \delta}{2}} \tag{13}$$

$$\beta_u = \sqrt{\frac{k_u}{EA}} \tag{14}$$

Where k_u is the longitudinal equivalent elastic soil spring coefficient, x_u is the maximum elastic longitudinal deformation of equivalent elastic soil spring and δ is the ground displacement.

1.5 Reaction of pipelines to SWP

In the case of SWP (Fig. 3), it has been assumed that the pipeline moves with the ground and the displacement remains in elastic limit due to the wave amplitude is much smaller than the wave length. Depending on the above equations (Eqs. (7) and (8)), the maximum axial strains (ε_{au}, ε_{av}) and bending strain (ε_b) have been suggested for continuous pipelines as below

$$\varepsilon_{au} = \frac{\pi \overline{\delta}}{\lambda} \tag{15}$$

$$\varepsilon_{av} = 2\pi^2 \frac{\left(\overline{\delta}\right)^2}{\lambda^2} \tag{16}$$

$$\varepsilon_b = 2\frac{\overline{\delta} \pi^2}{\lambda^2} D \tag{17}$$

D is the outside diameter of the pipe, $\overline{\delta}$ is the wave amplitude and λ is the wave length.

1.6 Failure criteria of segmented pipelines and importance factor

The joint displacement of the segmented pipeline should be less than the allowable joint opening. Besides, as a

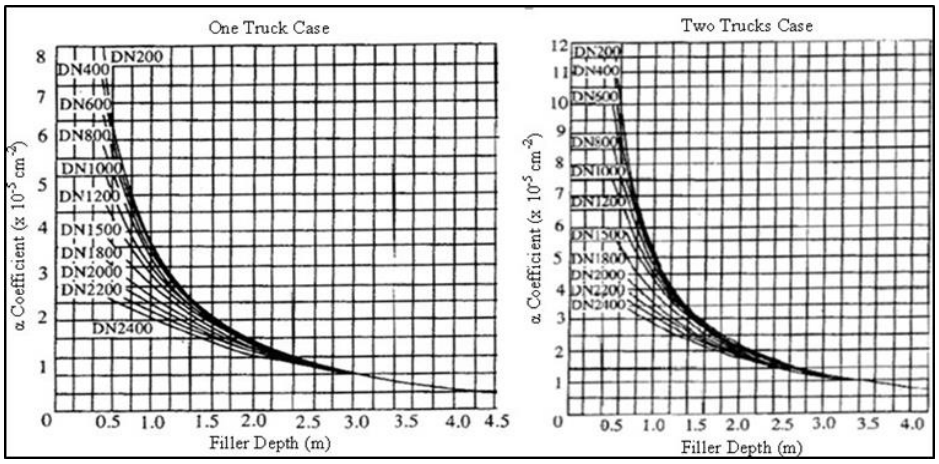

Fig. 4 α Coefficient (Turkdogan and Yetilmezsoy 2004)

Table 1 Importance factor for different classes of pipeline (Ip)

Class of pipeline	Wave propagation	Faulting	Transverse and Longitudinal PGD	Landslide
I	1.5	2.3	1.5	2.6
II	1.25	1.5	1.35	1.6
III	1.0	1.0	1.0	1.0
IV	Seismic conditions needn't be considered			

general approach, it is assumed that the tolerable relative joint opening of the segmented pipeline is approximately half of the total joint depth (O'Rourke and Liu 1999).

The amount of design seismic hazard for any pipeline classes may be obtained by multiplying the importance factor (I_p). This factor has been described by The Indian Institute of Technology Kanpur (IITK 2007) as in Table 1 according to failure cases (IITK 2007).

Class-I includes very essential water pipelines and high pressure (≥10 kgf/cm^2) oil and gas pipelines. Class-II is expressed as critical water pipelines and medium pressure (between 3 kgf/cm^2 and 10 kgf/cm^2) oil and gas pipelines. Class-III contains the water supply pipelines for ordinary use and low pressure (≤3 kgf/cm^2) oil and gas pipelines. Class-IV is described as low or very little importance water pipelines (IITK 2007).

1.7 Additional strain

Buried pipelines may have additional strain due to soil (filler) weight, traffic load, temperature change and operating pressure. All of these additional effects should be considered in terms of the seismic analyses of buried pipelines. However, in this study, since the segmented (sewage or stormwater) pipelines examined have no inner pressure, the operating pressure and water-hammer effects have not been taken into account.

1.7.1 Additional strain due to soil (Filler) weight

External pressure due to soil (filler) weight can be calculated as below

$$P_0 = \gamma H \frac{1 + k_0}{2} \tag{18}$$

Where H is the depth to center-line of the pipeline γ is the unit weight of soil (filler), k_o is the coefficient of lateral soil pressure at rest. Due to backfilling and compaction of the soil around buried pipelines, O'Rourke *et al*. (1985) has recommend that k_o=1.0 (O'Rourke *et al*. 1985).

1.7.2 Traffic load

The soil pressure (W_t) caused by the traffic load can be calculated using the Boussinesq method as follows

$$W_t = F\alpha P \tag{19}$$

F is the effect coefficient (can be taken as 1.5), α is the Boussinesq coefficient that described in the figure (Fig. 4), P is the wheel load and for heavy traffic this value can be taken as 10.000 kgf (Turkdogan and Yetilmezsoy 2004).

1.7.3 Temperature change

Soil surface temperature can change significantly at different times of a day. If this change affects the depth of the soil and reaches the buried pipeline, this effect must be taken into consideration, as well. On the other hand, sometimes buried pipelines may have different temperature values before and after the commissioning. This temperature change causes additional stresses, deformations and strains in the pipelines. All of these effects can be calculated using the following known equation

$$\varepsilon_t = \alpha(T_2 - T_1) \tag{20}$$

Where α is the coefficient of thermal expansion, $\Delta T = T_2 - T_1$ is the temperature difference and $\varepsilon_t$is the strain due to temperature change.

2. Regional geology and seismicity

The investigated region is located on the Shore of the Marmara Sea in Southern Istanbul (Fig. 5). In this landslide-prone area Gurpinar and Cukurcesme soil formations are predominant. Critical acceleration (a_c) values for Cukurcesme formation range between 0.20 g-0.55 g and for Gurpinar formation are in between 0.6 g-0.8 g. Besides, it is understood from the previous surveys

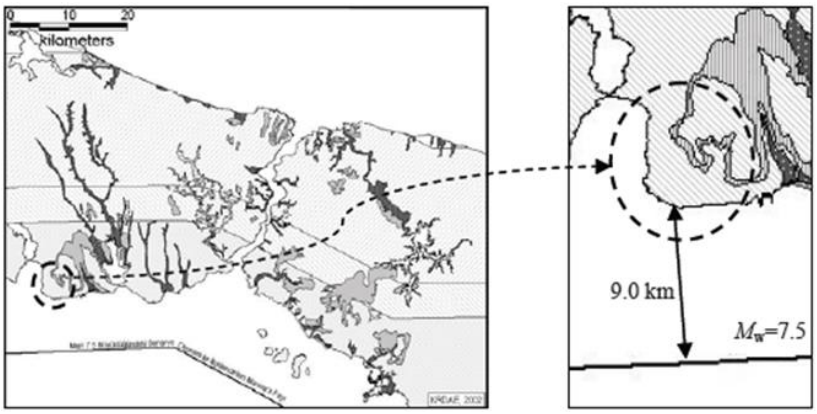

Fig. 5 Investigated region and North Anatolian fault (Yigit *et al*. 2018)

Table 2 Properties of the investigated pipe and pipeline

Concrete Pipe	Outside Diameter (mm)	Pipe Length, *L*0 (mm)	Wall Thickness, *t* (mm)	Joint Depth, *d* (mm)	Compressive Design Strength (kN/cm^2)	Depth, *H* (cm)
Ø300	400	1580	50	80	2.0	450

that some inclined areas have slope angles up to 40° (Merka 2006). On the other hand, the smallest wavelength in this region has been obtained as 90 m (Gedikli *et al*. 2008).

North Anatolian Fault Zone (NAFZ) is an active strike-slip fault line that runs south of Istanbul, throughout Marmara Sea (Fig. 4). The distance between the examined area and the fault line is approximately R=9.0 km and a major earthquake is expected with a Richter moment magnitude of about 7.5.

3. Characteristics of segmented pipelines in the region

Segmented pipelines generally use for the construction of sewage and/or stormwater networks. These systems have no inner pressure and flow occurs due to the inclination of the segmented pipeline networks. Therefore, depending on this inclination, the depth of the buried segmented pipelines is variable. Investigations have been carried out on the concrete pipeline widely used in the region and whose characteristics are given in the table (Table 2).

The pipelines have been constructed with concrete cylinder pipes with rubber gasketed joints. Therefore, pipe material is concrete and the properties of the investigated segmented pipe widely used in this region are as in Table 2.

It is determined that the trench, and hence the surround of the pipe, has been filled with crushed stone (γ=1800 kgf/m^3, Ø=36°). It means that the filler-pipe interface is concrete and the filler is cohesionless material (c=0).

4. Solution

Buried pipelines have been the main subject of many studies. Some of them have examined the fault line-pipeline intersection issue, some of them have investigated the pipeline-soil interaction, and some of them have focused on seismic wave propagation-pipeline interaction.

Some research methods are analytical while others are numerical or experimental (Yun and Kyriakides 1990, Vazouras *et al*. 2010, Vazouras *et al*. 2012, Vazouras *et al*. 2015, Mina *et al*. 2020, Triantafyllaki *et al*. 2020, Forcellini *et al*. 2020, Alexoudi e al. 2007, Shi 2015b, Wang 1979, O'Rourke and Bouabid 1996, El Hmadi and O'Rourke 1990, Bouabid 1995). In this study, as in the mentioned approach (section 1.3), the behavior of segmented buried pipeline subject to permanent ground deformation (PGD) has been examined as two parts, as well. According to transverse and longitudinal PGD cases, solutions have been obtained as explained in section 4.1. The fault line-pipeline intersection case has not been studied since there is no fault line-pipeline intersection in this investigated area. On the other hand, the seismic wave propagation case has been examined as another problem in section 4.2 for segmented pipelines.

4.1 Response of segmented pipelines to PGD

Similar to the response of continuous pipelines, for the determination of the behavior of segmented pipelines the amount of permanent ground movement has a decisive role. Depending on this deformation, to obtain the response of the segmented pipelines to PGD, the problem has been described as a beam on elastic soil foundation with built-in supports at both ends and hinges at joints (Fig. 5). Therefore, two main conditions arise as transverse and longitudinal PGD effects.

4.1.1 Transverse permanent ground deformation case

Assuming that the pipe material remains within the elastic boundary, elastic beam theory has been applied as described in the figure (Fig. 6).

According to this approximation, the total maximum opening at one side of a joint is the sum of the axial pull-out plus rotation effect. When Eq. (9) is considered, it is understood that the largest rotation (Eq. (21)) and axial

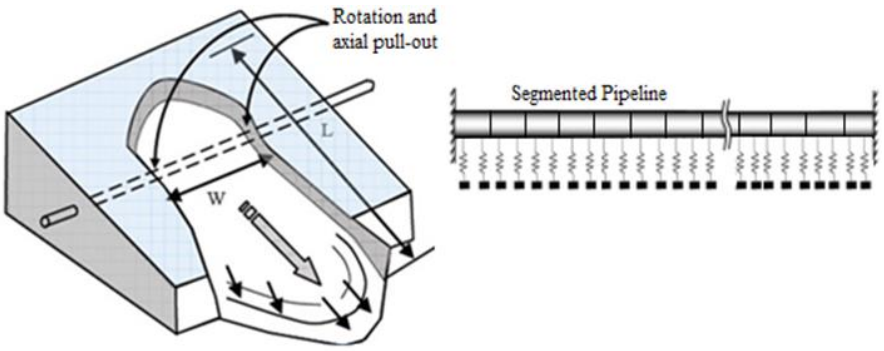

Fig. 6 Transverse PGD case model

extension (Eq. (10)) occur at x=0.

$$\theta = \frac{\beta_v \delta}{2} \tag{21}$$

Depending on this equation (Eq. (21)), the maximum opening due to rotation has been obtained as below

$$\Delta d_r = \frac{\beta_v \delta}{2} D \tag{22}$$

The maximum pull-out of the joint at x=0 is as Eq. (23)

$$\Delta d_{at} = \varepsilon_{at} l_0 \tag{23}$$

At the end of the sum of Eq. (22) and Eq. (23), the total maximum opening of the joint (for x=0) has been obtained as follows

$$\Delta d_t = \Delta d_r + \Delta d_{at} \tag{24}$$

The maximum total opening of the joint must be less than the allowable joint extension. Where D is the outside diameter of the pipe, l_0 is the length of a pipe segment, δ is the ground displacement, ε_{at} is the maximum axial strain due to transverse PGD case (Eq. (10)) and β_v is explained as Eq. (12). Assuming that equivalent soil springs remain elastic, coefficient of soil spring (k_v) can be described as follows (ASCE 1984)

$$k_v = \frac{2p_u}{y_u} \tag{25}$$

For cohesionless soil (filler)

$$P_u = \bar{\gamma} H N_{qh} D \tag{26}$$

$$y_u = \begin{cases} (0.07\sim0.10)(H + D/2) & loose \\ (0.03\sim0.05)(H + D/2) & medium \\ (0.02\sim0.03)(H + D/2) & dense \end{cases} \tag{27}$$

Where N_{qh} is the horizontal bearing capacity of the filler material, D is the outside diameter of the pipe; H is the depth to center-line of the pipe and $\bar{\gamma}$ is the effective unit weight of the soil (filler).

4.1.2 Longitudinal permanent ground deformation case

This problem can be described as a beam on elastic soil foundation with built-in supports at both ends (Fig. 7). Besides, this beam has axial load due to the effects of longitudinal ground displacement. Under these circumstances, the maximum axial opening occurs at x=0 and the amount of this extension can be explained as below

$$\Delta d_{al} = \varepsilon_{al} l_0 \tag{28}$$

The parameters that ε_{al} (Eq. (13)) is dependent on can be defined as follows

$$k_u = \frac{2t_u}{x_u} \tag{29}$$

For cohesionless soil (filler)

$$t_u = \frac{\pi}{2} D \bar{\gamma} H (1 + k_0) \tan(k\emptyset) \tag{30}$$

Where D is the pipe outside diameter, $\bar{\gamma}$ is the effective unit weight of the soil (filler), H is the depth to center-line of the pipeline, Ø is the angle of shear resistance of the filler, k_0 is the coefficient of lateral soil pressure at rest and k is the reduction factor depending on the outer-surface characteristics of the pipe. k_0 can be obtained from Eq. (31) or Table 3 and k is defined as below (Table 4).

$$k_0 = 1 - \sin\emptyset \tag{31}$$

The maximum axial elastic deformation of equivalent elastic soil spring, x_u has been described as in the table (Table 5).

On the other hand, at the compression site concrete

Table 3 k_0 Values (Yigit 2015)

Soil	k_0
Loose	0.5-0.6
Dense	0.3-0.5
Clay (Drained)	0.5-0.6
Clay (undrained)	0.8-1.1
Compacted	1.0-1.3

Table 4 k Values (Yigit 2015)

Outer Surface of Pipe	k
Concrete	1.0
Tar	0.9
Stiff Steel	0.8
Smooth Steel	0.7
Epoxy	0.6
Polythene	0.6

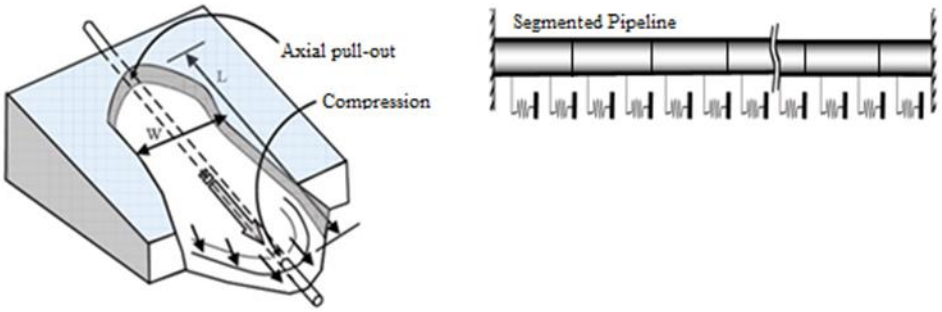

Fig. 7 Longitudinal PGD case model

Table 5 X_u Displacement ($\times 10^{-3}$m) (Yigit 2015)

	Lose	Medium	Dense
Sand	5	4	3
Clay	10	9	8

pipes can be damaged by compression force at joint. The maximum compressive stress at the joint subjected to maximum pressure stress can be calculated as Eq. (32)

$$\sigma = \frac{t_u L}{2A_{pipe}} \tag{32}$$

A_{pipe} is the pipe cross-section area and L is the length of the PGD zone. This value (σ) should not exceed the safety limit of the material.

4.2 Response of segmented pipelines to SWP

Ground displacement due to seismic wave propagation has been explained as two parts (section 1.2). For the perpendicular component, the total maximum opening of the joint can be explained as the sum of the axial pull-out and the rotation effect. In this situation (perpendicular direction case), the maximum axial opening occurs at x=0 and it can be defined as follows

$$\Delta d_{av} = \varepsilon_{av} l_0 \tag{33}$$

Besides; the largest rotation occurs at this point (x=0) for Ø=0 (Fig. 2) and it can be described as the following equation

$$\theta_{rv} = 2\pi \frac{\overline{\delta}}{\lambda} \tag{34}$$

The maximum opening due to rotation has been obtained as below

$$\Delta d_{rv} = D\theta_{rv} \tag{35}$$

According to perpendicular direction case, the total pull-out can be calculated from Eq. (36)

$$\Delta d_{vt} = \Delta d_{av} + \Delta d_{rv} \tag{36}$$

On the other hand, for the longitudinal direction (axial component) the maximum axial extension occurs at x=0 and it has been defined as follows

$$\Delta d_{au} = \varepsilon_{au} l_0 \tag{37}$$

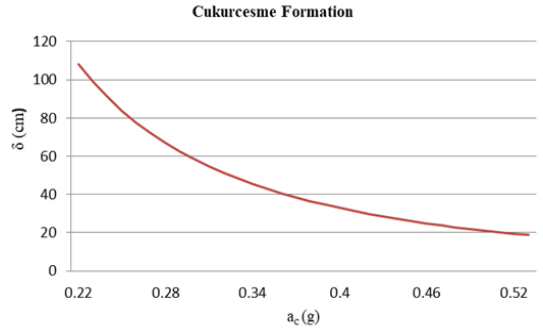

Fig. 8 δ-a_c Relation for Cukurcesme formation

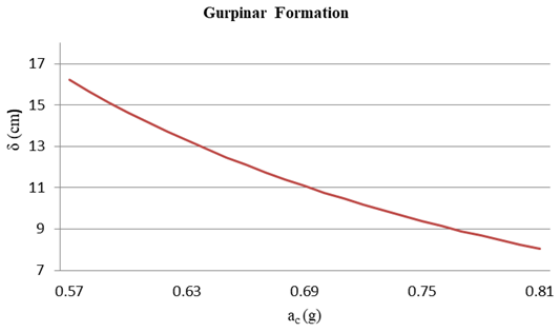

Fig. 9 δ-a_c Relation for Gurpinar formation

5. Analyses and results

5.1 Determination of amount of PGD

According to Eq. (1), ground displacement due to an earthquake can be calculated depending on the logarithmic values of Arias Intensity and critical acceleration. Considering the expected Istanbul Earthquake (M=7.5 and R=9 km, Fig. 4), Arias Intensity has been calculated from Eq. (2) as $\log I_a = 1.492$ m/s for the investigated region. Besides; for this area, the critical acceleration values of Cukurcesme and Gurpinar ground formations are between 0.22 g-0.53 g and 0.57 g-0.81 g, respectively (Siyahi *et al.* 2003). Based on these data, for $\log I_a$ value of 1.492 m/s, the relationship between critical acceleration (a_c) and ground displacement (δ) has been obtained for each examined formation (Figs. 8 and 9).

When the above figures are examined, it can be seen that Cukurcesme formation gives more ground displacement than Gurpinar formation. Therefore, considering Cukurcesme formation zone which has slope

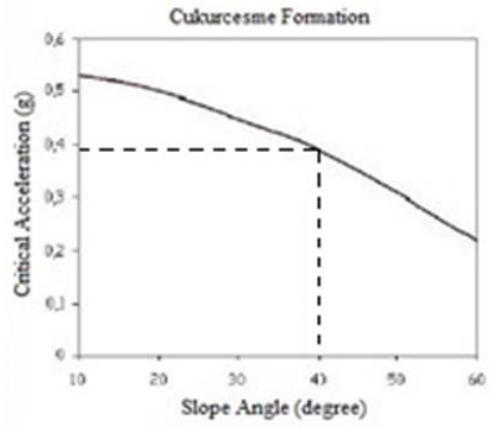

Fig. 10 Slope angle-ac relation for Cukurcesme formation (Siyahi *et al*. 2003)

Table 6 Results for transverse PGD case

Transverse PGD Case	y_u (m)	0.135
	γ (kN/m^3)	18
	N_{qh} (Ø=36^0)	22
	P_u (kN/m)	681.12
	k_v (kN/m^2)	10,091
	E (kN/m^2)	32,000,000
	β_v (1/m)	0.550
	δ (m)	0.35
	$I_{p\text{-}PGD}$ (Class-II)	1.35
	δ_{design} (m)	0.47
	ε_{at}	0.008
	Δd_{at} (cm)	1.3
	Δd_r (cm)	5.2
	Δd_t (cm)	**6.5**

Table 7 Results for longitudinal PGD case

Longitudinal PGD Case	x_u (m)	0.004
	t_u (kN/m) (Ø=36°)	52.22
	k_u (kN/m^2)	26,108
	β_u (1/m)	0.122
	δ (m)	0.35
	$I_{p\text{-}PGD}$ (Class-II)	1.35
	δ_{design} (m)	0.47
	ε_{al}	0.004
	Δd_{al} (cm)	**0.6**

angles up to 40°, the critical acceleration has been obtained as 0.39 g as shown in Fig. 10.

For the critical value of 0.39 g and $\log I_a$ value of 1.492 m/s, ground displacement has been calculated from Eq. (1) as δ=35 cm. On the other hand, considering Eq. (5), the wave amplitude, $\bar{\delta}$, has been calculated as 66 cm.

5.2 Analyses of the segmented pipelines subject to PGD and SWP

Calculations have shown that additional deformations due to traffic load, temperature change and soil pressure are negligible for the investigated case. According to transverse PGD case obtained results have been given in Table 6. As a result, the total joint opening has been calculated as 6.5 cm for this situation (Transverse PGD).

Table 8 Results for SWP case

SWP Case	$\bar{\delta}$ (cm)	0.66
	$I_{p\text{-}swp}$ (Class-II)	1.25
	$\bar{\delta}_{design}$ (cm)	0.83
	λ (m)	90
	ε_{av}	0.002
	ε_{au}	0.029
	Δd_{av} (cm)	0.3
	Δd_{rv} (cm)	2.3
	Δd_{vt} (cm)	**2.6**
	Δd_{au} (cm)	**4.6**

On the other hand, depending on the earthquake-induced ground displacement, the other important problem is longitudinal PGD case, as well. For this case the joint opening has been obtained as 0.6 cm (Table 7).

According to the seismic wave propagation case, the data used and the obtained results are as in Table 8. The maximum axial pull-out due to the perpendicular component of the seismic wave has been calculated as 2.6 cm. Besides, the axial opening caused by the longitudinal component of the seismic wave has been obtained as 4.6 cm.

Here, each case has been examined separately. However, as an example, if PGD occurs in addition to SWP, a combination of two conditions should be considered for the solution. Depending on these outcomes, to compare the safety of the segmented pipeline, it has been assumed that the allowable joint opening (d_a) is half of the total joint depth. Therefore, the tolerable joint extension of the investigated pipeline has been taken as $d_a=d/2$=4.0 cm. According to this allowable value, for the investigated segmented pipeline, the failure criterion has been exceeded in the cases of transverse PGD and SWP. On the other hand, considering the allowable joint opening of the examined pipeline (4 cm), the bearable PGD amount has been calculated as approximately 23 cm for the transverse case and $\bar{\delta}/\lambda$ proportion has been obtained as 0.64% for SWP case.

Depending on the Eq. (32), in the compression region, the length of the examined pipeline which could be exposed to PGD has been calculated as L_{PGD}=42 m. In other words, for the longitudinal PGD case, if the length of the investigated segmented pipeline in the PGD zone exceeds 42 m, pressure damages to the pipeline may occur.

Under the same circumstances, to investigate the behaviors of the segmented pipelines for different diameters Table 9 has been prepared. According to this table, the transverse PGD case has a decisive role in seismic safety of buried segmented pipelines. Besides, it can be seen that L_{PGD} increases as the pipe diameter increases based on these pipe features.

In the case of SWP, for Ø200 pipe limit value is exceeded (Δd_{au}=3.8 cm>d_a=3.0 cm). On the other hand, the ratio of wave amplitude ($\bar{\delta}$) to wavelength (λ) is another

Table 9 Results for various pipe diameters

Pipe	D (m)	L_0 (m)	t (m)	Δd_t (cm)	Δd_{al} (cm)	Δd_{vt} (cm)	Δd_{au} (cm)	d_a (cm)	L_{PGD} (m)
Ø200	0.276	1.310	0.038	6.6	0.6	1.8	3.8	3	32
Ø400	0.510	1.335	0.055	6.2	0.5	3.2	3.9	4.25	47
Ø500	0.624	1.340	0.062	6.2	0.4	3.8	3.9	4.5	54
Ø600	0.740	1.340	0.070	6.3	0.4	4.5	3.9	4.5	61

important parameter. If this rate increases, SWP will be more effective on the buried pipelines.

6. Conclusions

Investigation of behavior of buried pipelines subject to earthquake effects is one of the most important subjects of structural engineering. In this paper, as a part of the seismic study of a special area in Istanbul, the case of segmented pipelines under earthquake effects has been examined. Analytical solution has been preferred to acquire practical and useful equations for the general approach. Based on the mathematical models prepared in this research, new appropriate equations that calculate the response of buried pipelines subject to earthquake effects have been obtained.

The examined area has very high landslide risks. Especially, considering the expected Istanbul Earthquake, it can be said that this region is not available for settlement. Due to this earthquake, beside superstructures, infrastructures can get damaged, as well. In this study, buried segmented pipelines commonly used in this investigated zone have been examined and obtained results show that probable seismic hazards, especially due to earthquake-induced ground movement effects, are very high.

According to obtained results, using segmented pipes which have a larger allowable joint opening capacity may reduce these negative effects. To mitigate the seismic effects, pipe-soil interface material with a low friction coefficient, such as polythene, should be used. Moreover, filler material with a low friction coefficient, less soil depth, pipe with thick wall, pipe material with higher elasticity modulus and filler material with low unit weight may decrease these damages, as well. It has been determined that considering all these applications in practice will be beneficial in reducing the effects of the earthquake on segmented pipelines.

References

Alexoudi, M., Terzi, V. and Chatzigogos, T. (2007), "Numerical assessment of damage state of segmented pipelines due to permanent ground deformation", *Proceeding of 10th International Conference on Applications of Statistics and Probability in Civil Engineering*, Tokyo, Japan, July.

American Society of Civil Engineers (ASCE) (1984), "Guidelines for the seismic design of oil and gas pipeline systems", Committee on Gas and Liquid Fuel Lifeline, ASCE.

Apak, M.Y., Ozen, H., Calıc, M., Golgeli, B. and Ataoglu, S. (2022), "Applications of utility tunnels for natural gas pipelines", *Tunnel. Underg. Space Technol.*, **122**, 104243. https://doi.org/10.1016/j.tust.2021.104243.

Banushi, G. and Wham, B.P. (2021), "Deformation capacity of buried hybrid-segmented pipelines under longitudinal permanent ground deformation", *Can. Geotech. J.*, **58**(8), 1095-1117. https://doi.org/10.1139/cgj-2020-0049.

Bouabid, J. (1995), "Behavior of rubber gasketed concrete pipe joints during earthquakes", Ph.D. Thesis, Rensselaer Polytechnic Institute, December.

Castiglia, M., Magistris, F.S. and Napolitano, A. (2018), "Stability of onshore pipelines in liquefied soils: Overview of computational methods", *Geomech. Eng.*, **14**(4), 355-366. http://doi.org/10.12989/gae.2018.14.4.355.

El Hmadi, K. and O'Rourke, M.J. (1990), "Seismic damage to segmented buried pipelines", *Earthq. Eng. Struct. Dyn.*, **19**(4), 529-539. https://doi.org/10.1002/eqe.4290190405.

Forcellini, D., Mina, D. and Karampour, H. (2022), "The role of soilstructure interaction in the fragilityassessment of HP/HT unburiedsubsea pipelines", *J. Marine Sci. Eng.*, **10**(1), 110. https://doi.org/10.3390/jmse10010110.

Gedikli, A., Lav, M.A. and Yiğit, A. (2008), "Seısmıc vulnerability of a natural gas pipeline network", *ASCE Pipelines 2008*, Atlanta, July.

Gregor, N.J. (1995), "The attenuation of strong ground motion displacements", Earthquake Engineering Research Center, Report Number UCB/EERC-95/02, University of California at Berkeley, June.

Hsieh, S. and Lee, C.T. (2011), "Empirical estimation of the Newmark displacement from the Arias intensity and critical acceleration", *Eng. Geology*, **122**, 34-42. https://doi.org/10.1016/j.enggeo.2010.12.006.

Indian Institute of Technology Kanpur (2007), IITK-GSDMA Guidelines for Seismic Design of Buried Pipelines, November.

Jibson, R.W. (1993), "Predicting earthquake-induced landslide displacements using Newmark's sliding block analysis", *Transp. Res. Record*, **1411**, 9-17.

Jibson, R.W. (2007), "Regression models for estimating coseismic landslide displacement", *Eng. Geology*, **91**, 209-218. https://doi.org/10.1016/j.enggeo.2007.01.013.

Jibson, R.W., Harp, E.L. and Michael, J.M. (1998), "A method for producing digital probabilistic seismic landslide hazard maps: An example from the Los Angeles, California area", US Geological Survey Open-File Report 98-113.

Liu, L., Yang, C. and Wang, X. (2021), "Landslide susceptibility assessment using feature selection-based machine learning models", *Geomech. Eng.*, **25**(1), 1-16. http://doi.org/10.12989/gae.2021.25.1.001.

Londono, T.V. and O'Rouerke, M. (2018), "Influence of diameter on seismic response of buried segmented pipelines", *Soil Dyn. Earthq. Eng.*, **107**, 332-338. https://doi.org/10.1016/j.soildyn.2018.01.034.

Merka Insaat Taahhut Muhendislik Ticaret A.S. (2006), "Gurpınar-beylikduzu ve yakuplu beldeleri jeolojik ve jeofizik esasli etud raporu", Nisan, Istanbul, Türkiye. (in Turkish)

Mina, D., Forcellini, D. and Karampour, H. (2020), "Analytical fragility curves for assessment of the seismic vulnerability of hp/ht unburiedsubsea pipelines", *Soil Dyn. Earthq. Eng.*, **137**, 106308. https://doi.org/10.1016/j.soildyn.2020.106308.

Nanahkaran, Y.A., Mao, Y., Azarafza, M., Kockar, M.K. and Zhu,

H. (2021), "Fuzzy-based multiple decision method for landslide susceptibility and hazard assessment: A case study of Tabriz, Iran", *Geomech. Eng.*, **24**(5), 407-418. http://doi.org/10.12989/gae.2021.24.5.407.

Newmark, N.M. (1965), "Effects of earthquakes on dams and embankments", *Geotechnique*, **15**, 139-159. http://doi.org/10.12989/gae.2021.24.5.407.

O'Rourke, M. (1989), "Approximate analysis procedure for permanent ground deformation effect on buried pipelines", *Proceedings of 2nd Japan-U.S. Workshop on Liquefaction, Large Ground Deformation and Their Effects on Lifeline Facilities*, Buffalo, New York.

O'Rourke, M. and Bouabid, J. (1996), "Analytical damage estimates for concrete pipelines", *Proceedings of Eleventh World Conference on Earthquake Engineering*, Acapulco, Mexico, June.

O'Rourke, M. and Londono, T.V. (2016), "Analytical model for segmented pipe response to tensile ground strain", *Earthq. Spectra*, **32**(4), 2533. http://doi.org/10.1193/050415EQS064M.

O'Rourke, M.J. and Liu, X. (1999), "Response of buried pipelines subject to earthquake effects", Monograph No. 3, Multidisciplinary Center for Earthquake Research, University of Buffalo, Buffalo.

O'Rourke, T.D., Grigoriu, M.D. and Khater, M.M. (1985), "A state of the art review: seismic response of buried pipelines", Ed. C. Sundararajan, Decade of Progress in Pressure Vessel Technology, ASME.

Shi, P. (2015a), "Surface wave propagation effects on buried segmented pipelines", *J. Rock Mech. Geotech. Eng.*, **7**(4), 440-451. https://doi.org/10.1016/j.jrmge.2015.02.011.

Shi, P. (2015b), "Seismic wave propagation effects on buried segmented pipelines", *Soil Dyn. Earthq. Eng.*, **72**, 89-98. https://doi.org/10.1016/j.soildyn.2015.02.006.

Siyahi B., Erdik M., Sesetyan K., Demircioglu M.B. and Akman H. (2003), "Sıvılasma ve sev stabilitesi hassaslıgı ve potansiyeli haritaları:istanbul örnegi", *Besinci Ulusal Deprem Muhendisligi Konferansı*, Istanbul, Türkiye. (in Turkish)

Toprak, S., Nacaroglu, E. and Koc, C.A. (2015), "Seismic damage probabilities for segmented buried pipelines in liquefied soils", *6th International Conference on Earthquake Geotechnical Engineering*, Christchurch, New Zealand.November.

Toprak, S., Nacaroglu, E., Ballegooy, S.V., Koc, C.A., Jacka, M., Manav, Y., Torvelainen, E. and O'Rourke, T.D. (2019), "Segmented pipeline damage predictions using liquefaction vulnerability parameters", *Soil Dyn. Earthq. Eng.*, **125**, 105758. https://doi.org/10.1016/j.soildyn.2019.105758.

Triantafyllaki, A., Papanastasiou, P. and Loukidis, D. (2020), "Numerical analysis of the structural response of unburied offshore pipelines crossing active normal and reverse faults", *Soil Dyn. Earthq. Eng*., **137**, 106296. https://doi.org/10.1016/j.soildyn.2020.106296.

Turkdogan, F.İ. and Yetilmezsoy, K. (2004), "Su getirme ve kanalizasyon uygulamaları", Su Vakfı Yayınları, Istanbul, Türkiye. (in Turkish)

Vazouras, P., Dakoulas, P. and Karamanos, S.A. (2015), "Pipe-soil interaction and pipeline performance under strike-slip fault movements", *Soil Dyn. Earthq. Eng*., **72**, 48-65. https://doi.org/10.1016/j.soildyn.2015.01.014.

Vazouras, P., Karamanos, S.A. and Dakoulas, P. (2010), "Finite element analysis of buried steel pipelines under strike-slip fault displacements", *Soil Dyn. Earthq. Eng*., **30**, 1361-1376. https://doi.org/10.1016/j.soildyn.2010.06.011

Vazouras, P., Karamanos, S.A. and Dakoulas, P. (2012), "Mechanical behavior of buried steel pipes crossing active strike-slip faults", *Soil Dyn. Earthq. Eng*., **41**, 164-180. https://doi.org/10.1016/j.soildyn.2012.05.012.

Wang, L.R.L. (1979), "Some aspects of seismic resistant design of buried pipelines", Lifeline Earthquake Engineering-Buried Pipelines, Seismic Risk, and Instrumentation, PVP-34, ASME.

Wang, T., Zhou, G., Wang, J. and Wang, D. (2020), "Impact of spatial variability of geotechnical properties on uncertain settlement of frozen soil foundation around an oil pipeline", *Geomech. Eng.,* **20**(1), 19-28. http://doi.org/10.12989/gae.2020.20.1.019.

Wham, B.P. and Davis, A.C. (2019), "Buried continuous and segmented pipelines subjected to longitudinal permanent ground deformation", *J. Pipeline Syst. Eng. Pract.*, **10**(4), 04019036. https://doi.org/10.1061/(ASCE)PS.1949-1204.0000400.

Wham, B.P., Franke, K.W., Dashti, S. and Kayen, R.E. (2017), "Water supply damage caused by the 2016 Kumamoto Earthquake", *Lowland Technol. Int.*, **19**(3), 151-160.

Wijaya, H., Rajaev, P. and Gad, E. (2019), "Effect of seismic and soil parameter uncertainties on seismic damage of buried segmented pipeline", *Transp. Geotech.*, **21**, 100274. https://doi.org/10.1016/j.trgeo.2019.100274.

Wilson, R.C. and Keefer, D.K. (1983), "Dynamic analysis of a slope failure from the 6 August 1979 Coyote Lake, California, earthquake", *Bull. Seismol. Soc. Am.*, **73**(3), 863-877. https://doi.org/10.1785/BSSA0730030863.

Xie, J., Zhang, L., Zheng, Q., Liu, X., Dubljevic, S. and Zhang, H. (2021), "Strain demand prediction of buried steel pipeline at strike-slip fault crossings: A surrogate model approach", *Earthq. Struct.,* **20**(1), 109-122. http://doi.org/10.12989/eas.2021.20.1.109.

Yigit, A. (2015), "Buried continuous pipelines under the effects of earthquake", PhD Thesis, Istanbul Technical University, September, Istanbul, Turkey.

Yiğit, A. (2020), "Prediction of amount of earthquake-induced slope displacement by using newmark method", *Eng. Geology*, **264**, 105385. https://doi.org/10.1016/j.enggeo.2019.105385.

Yiğit, A. (2021), "Newmark yöntemine göre zemin deplasmanının tahmin edilmesi", *Politeknik Dergisi*, 1-1. http://doi.org/10.2339/politeknik.665258.

Yigit, A., Lav, M.A. and Gedikli, A. (2018), "Vulnerability of natural gas pipelines under earthquake effects", *J. Pipeline Syst. Eng. Pract.*, **9**(1), 04017036. https://doi.org/10.1061/(ASCE)PS.1949-1204.0000295.

Yoon, S., Lee, Y. and Jung, H. (2020), "A comprehensive approach to flow-based seismic risk analysis of water transmission network", *Struct. Eng. Mech.*, **73**(3), 339-351. http://doi.org/10.12989/sem.2020.73.3.339.

Yun, H. and Kyriakides, S. (1990), "On the beam and shell modes of buckling of buried pipelines", *Soil Dyn. Earthq. Eng*., **9**, 179-193. https://doi.org/10.1016/S0267-7261(05)80009-0.

Zhang, D., Bie, X., M., Zeng, X., Lei, Z. and Du, G.F. (2020), "Experimental and numerical studies on mechanical behavior of buried pipelines crossing faults", *Struct. Eng. Mech.*, **75**(1), 71-86. http://doi.org/10.12989/sem.2020.75.1.071.

CC